RADIATIONS FROM A CIRCULAR PATCH MICROSTRIP ANTENNA IN A TWO COMPONENT WARM PLASMA

DEEPAK BHATNAGAR and R. K. GUPTA
Department of Physics, M. R. Engineering College, Jaipur 302017, India.

ABSTRACT

Expressions for the electromagnetic and the electroacoustic field components of a circular patch microstrip antenna in a two-component warm plasma are obtained using linearized hydrodynamic theory and vector wave function techniques. The variation of the radiation conductance and the efficiency of the circular patch microstrip antenna with different ratios of plasma-to-source frequency is obtained and plotted. The values of radiation efficiency obtained in one-component and two-component warm plasma model are also compared.

INTRODUCTION

DUE to their light weight, better aerodynamic properties and low manufacturing cost, microstrip antennas are increasingly being used on aerospace vehicles, satellites and re-usable space shuttles[1-4]. An antenna mounted on a high flying high speed aerospace vehicle encounters ionized medium and its radiation properties are modified. Gujar and Gupta[5,6] and Bhatnagar and Gupta[7] studied the radiation properties of microstrip antennas in a one-component ionized plasma medium and have noticed considerable plasma effect.

In this paper, the radiation properties of a circular patch microstrip antenna in a two-component warm plasma is studied. Expressions for the electromagnetic (EM) and the plasma (P) mode component are derived, computed and plotted. The variation of the EM mode and the P mode radiation conductance for various ratios of source-to-plasma frequency is shown in the graphical form. The values of radiation efficiency (η) are calculated and compared with the corresponding values of η for single component plasma. It is concluded that for better understanding, the effect of ions should also be considered.

RADIATION FIELD EXPRESSIONS

The circular microstrip antenna shown in figure 1 can be excited by a microstrip transmission line connected at the edge or by a coaxial line from the back at the plane $\varphi = 0$.

Amongst the various modes that may be excited in such an antenna are the TM_{nm} modes with respect to

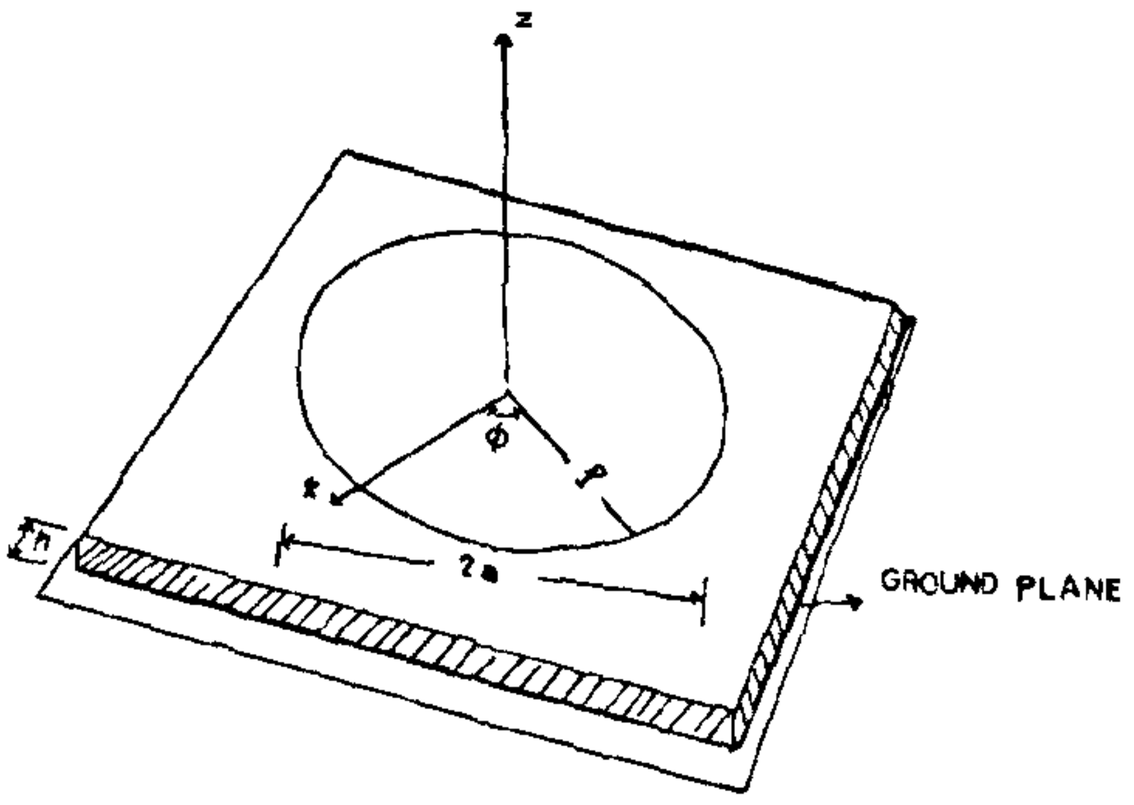

Figure 1. Geometry of circular patch microstrip antenna.

the z axis. The fields inside the cavity are obtained by[4]

$$E_z = k_1^2 J_n(k_1 \rho) \cos n\varphi. \quad (1)$$

For dominant reflection action at the circular dielectric to plasma medium boundary at $\rho = a$, the tangential magnetic field $H\varphi = jw \varepsilon_r k_1 J_n'(k_1 \rho)\cos n\varphi$ is very small and the values are given by

$$J_n'(k_1 a) = 0. \quad (2)$$

Following the method adopted by Bhatnagar and Gupta[7], Kumar and Gupta[8,9] and Talekar and Rawat[10], the EM and P mode fields are given by

EM mode fields:

$$E_\theta = \frac{k_1^2 \exp(-j\beta_e r) J_n(k_1 \rho) \beta_e (i)^n h}{2r}$$

$$J_n'(\beta_e a \sin\theta)\cos n\varphi, \quad (3)$$

$$E_\varphi = \frac{nk_1^2 \exp(-j\beta_e r) J_n(k_1\rho)\beta_e (i)^n h}{2r} \cos\theta \frac{J_n(\beta_e a \sin\theta)}{\beta_e a \sin\theta} \sin n\varphi. \quad (4)$$

P mode fields:

$$E_p = \sum_{j=1,2} (-2\pi) \frac{Ne(1-\alpha_j)(-\beta_{pj})k_1^2 n J_n(k_1\rho)h}{8\pi\omega\varepsilon_0 r} \times \frac{\sin(\beta_{pj} h\cos\theta)}{b_{pj} h\cos\theta} \times (-i)^n J_n(\beta_{pj} a\sin\theta) \times \sin n\varphi \exp(-j\beta_{pj} r)\left(\frac{\omega_{pe}^2}{NeA\omega^2} + \frac{\omega_{pe}^2}{NeA\omega^2} \times \frac{(\alpha_1+\alpha_2)}{(\alpha_1-\alpha_2)} + \frac{2\omega_{pi}^2}{NeA\omega^2(\alpha_1-\alpha_2)}\right), \quad (5)$$

where

$$A = \left(1 - \frac{\omega_{pe}^2}{\omega^2} - \frac{\omega_{pi}^2}{\omega^2}\right)$$

and

$$k_1 = \omega(\mu_0\varepsilon_0\varepsilon_r)^{\frac{1}{2}} \quad (6)$$

α_1 and α_2 are the roots of the equation

$$T_{21}\alpha_j^2 + (T_{11} - T_{22})\alpha_j - T_{12} = 0$$

$$T_{11} = \frac{\omega^2}{u_e^2}\left(1 - \frac{\omega_{pe}^2}{\omega^2}\right) \quad (7)$$

$$T_{12} = \omega_{pi}^2/u_i^2$$

$$T_{21} = \omega_{pe}^2/u_e^2,$$

$$T_{22} = \frac{\omega^2}{u_i^2}\left(1 - \frac{\omega_{pi}^2}{\omega^2}\right). \quad (8)$$

The wave numbers β_{pj} are given by the roots of the equations

$$\beta_{pj}^4 - (T_{11}+T_{22})\beta_{pj}^2 + (T_{11}T_{22} - T_{12}T_{21}) = 0 \quad (9)$$

and are related with α_j by

$$\beta_{pj}^2 = T_{11} + T_{21}\alpha_j. \quad (10)$$

The value of $|E_\theta|^2$ and $|E_\varphi|^2$ are computed for two-plasma frequencies and plotted in figures 2 and 3. The plasma mode field pattern $|E_p|^2$ for $A = 0.5$ is plotted in figure 4.

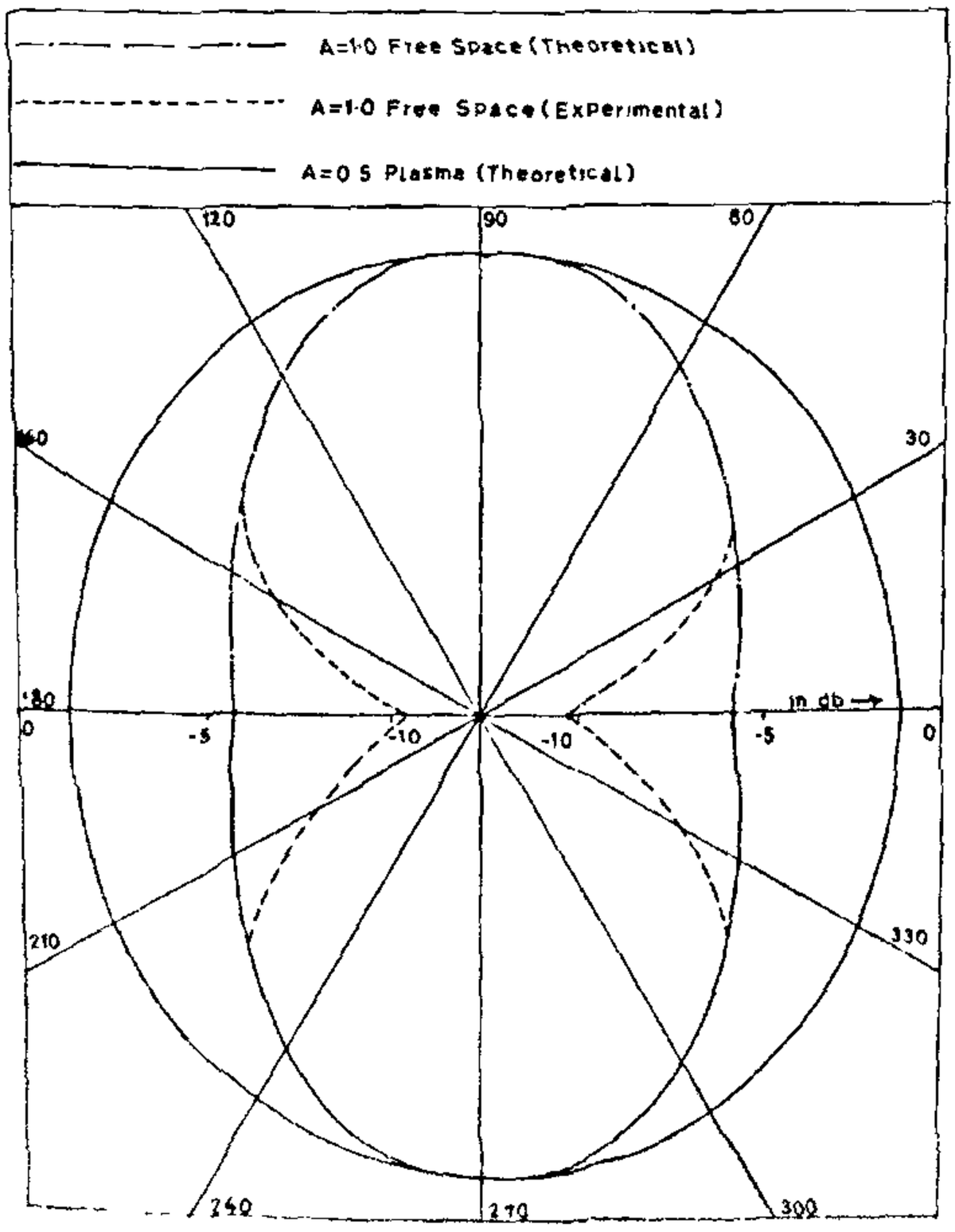

Figure 2. Variation of theoretical and experimental values of $|E_\theta|^2$ with plasma frequency.

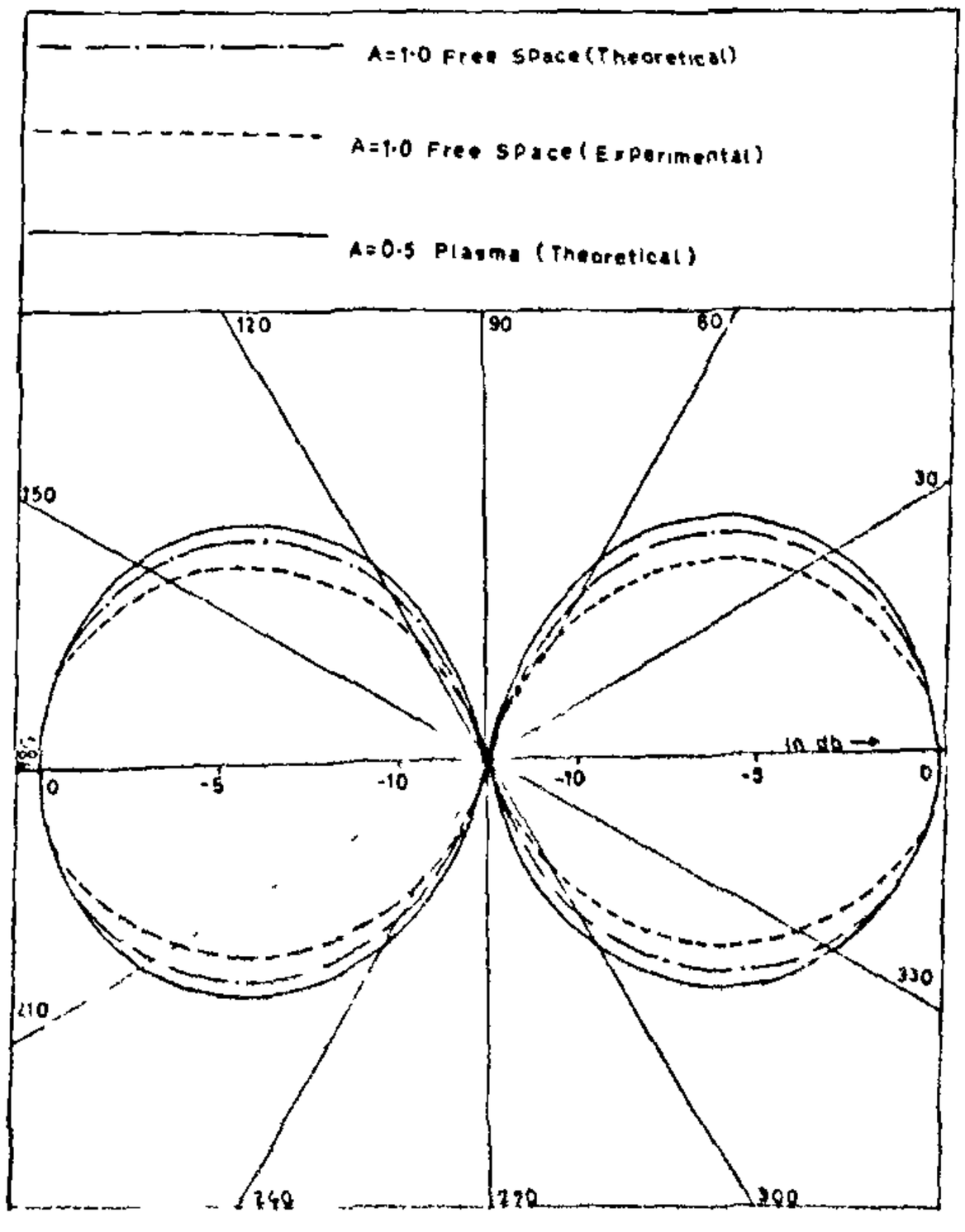

Figure 3. Variation of theoretical and experimental values of $|E_\varphi|^2$ with plasma frequency.

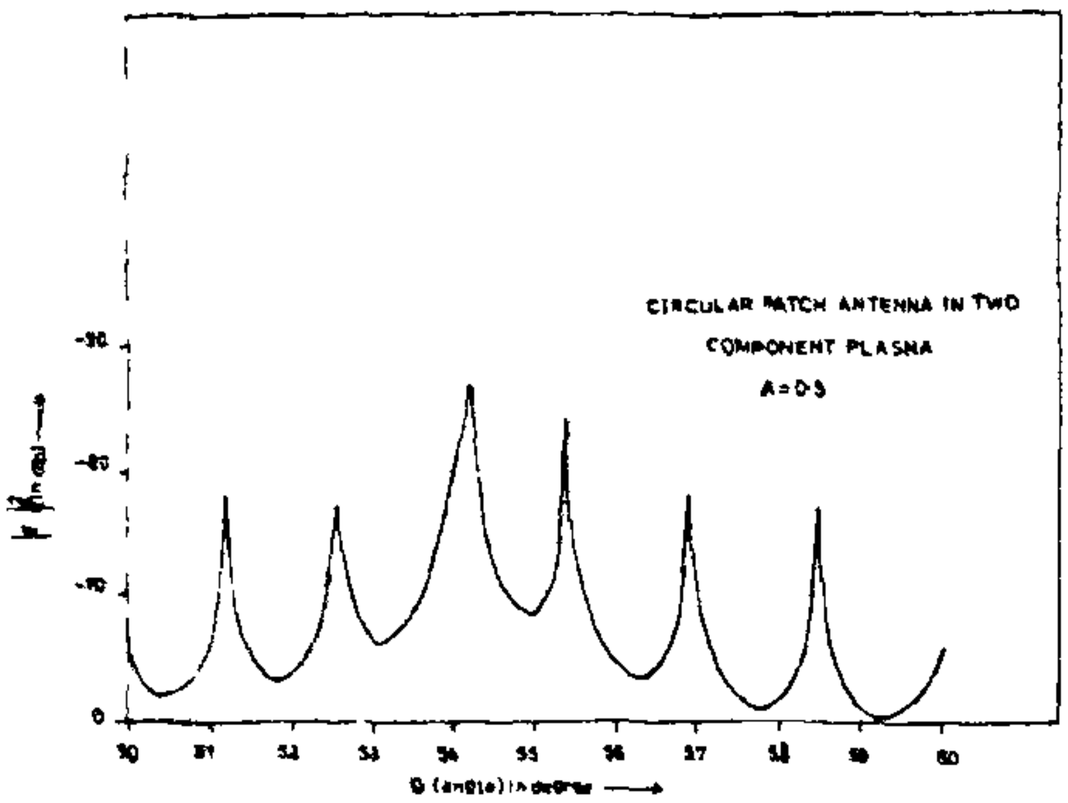

Figure 4. Variation of theoretical values of $|E_p|^2$ with plasma frequency for $A = 0.5$.

RADIATION CONDUCTANCE AND RADIATION EFFICIENCY

The radiation conductance G_e of the EM mode is given by

$$G_e = 2P_e/\iota_0^2 = \frac{(\beta_e a)^2}{960} I \qquad (11)$$

where

$$I = \int_0^{\pi} [\{J_{n-1}(\beta_e a \sin\theta) - J_{n+1}(\beta_e a \sin\theta\}^2 + [J_{n-1}(\beta_e a \sin\theta) + J_{n+1}(\beta_e a \sin\theta)]^2 \times \cos^2\theta] \sin\theta \, d\theta. \qquad (12)$$

Similarly G_p, the radiation conductance of the P mode is obtained as

$$G_p = \frac{2P_p}{\iota^2} = \sum_{j=1,2} \frac{(1-\alpha_j)^2 \omega_{pe}^2 \pi}{8\beta_{pj}(1+\tau\alpha_j^2)\omega u_e^2 \varepsilon_0} \int_0^{\pi} \left(J_1(\beta_{pj} a \sin\theta) \frac{\sin(\beta_{pj} h \cos\theta)}{\beta_{pj} h \cos\theta} \right)^2 \sin\theta \, d\theta. \qquad (13)$$

The value of G_e and G_p are plotted in figure 5. The radiation efficiency η is defined as[11]

$$\eta = \frac{P_e}{P_e + P_p} \times 100\,\%.$$

The variation of radiation efficiency of circular patch antenna in a one- and a two-component warm plasma with plasma frequency is plotted in figure 6, which also shows the variation of radiation efficiency of a half wave dipole.

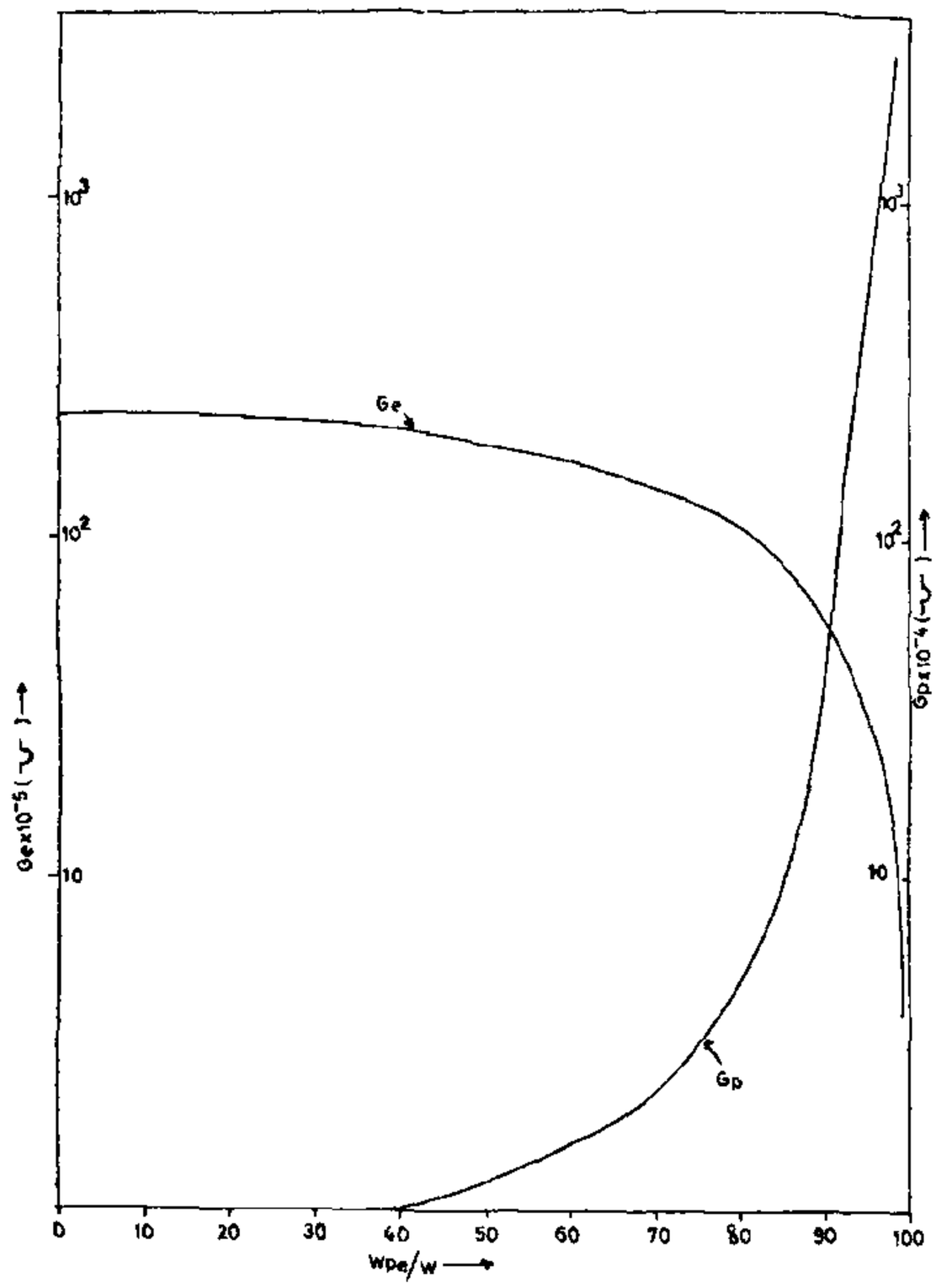

Figure 5. Variation of radiation conductances (G_e and G_p) with plasma frequencies.

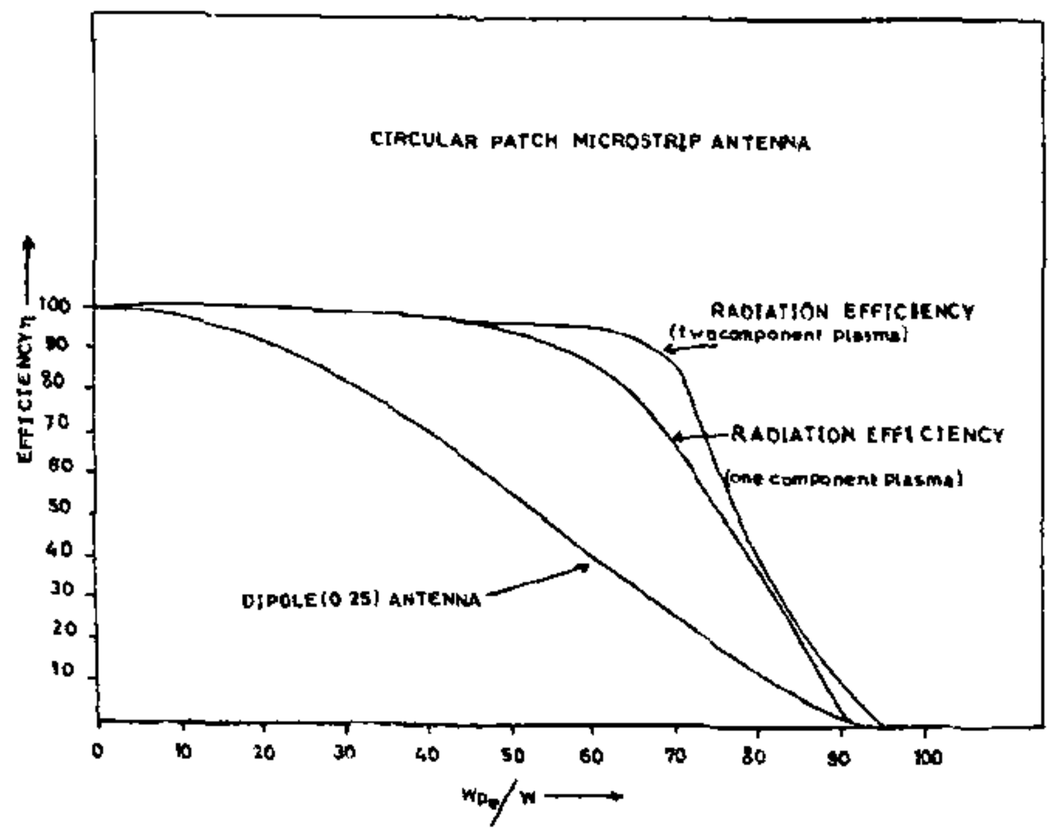

Figure 6. Variation of radiation efficiency of circular patch microstrip and $\lambda/2$ dipole antenna with plasma frequencies.

DISCUSSION AND CONCLUSION

From figures 2 and 3, it is obvious that the presence of plasma greatly affects the $|E_\theta|^2$ pattern. The patterns

become circular in this plane whereas half power beam width of $|E_\varphi|^2$ (figure 3) patterns increases in plasma.

The plot of $|E_p|^2$ as shown in figure 4 is similar to other microstrip and conventional antennas[5-9].

The radiation efficiency in a two-component plasma is greater as compared to a one-component plasma. However, it is substantially greater in comparison with half wave dipole.

ACKNOWLEDGEMENT

The authors are indebted to ISRO, Bangalore for providing the project grant and research fellowship to DB.

7 February 1985

1. Post, R. E. and Stephenson, D. T., *IEEE Trans. Ante. Propag.*, 1981, **29**, 129.
2. Carver, K. R. and Mink, J. W., *IEEE Trans. Ante. Propag.*, 1981, **29**, 2.
3. Derneryd, A. G., *IEEE Trans. Ante. Propag.*, 1977, **27**, 660.
4. James, J. R. and Wilson, G. J., *Microwaves optics and acoustics*, 1977, **1**, 165.
5. Gujar, N. K. and Gupta, R. K., *Curr. Sci.*, 1984, **53**, 561.
6. Gujar, N. K. and Gupta, R. K., *Indian J. Radio Space Phys.*, 1984, **13**, 125.
7. Bhatnagar, D. and Gupta, R. K., *J. Inst. Electron. Telecomn. Engrs.*, 1984, **30**, 92.
8. Kumar, A. and Gupta, R. K., *Curr. Sci.*, 1982, **51**, 689.
9. Kumar, A. and Gupta, R. K., *Curr. Sci.*, 1983, **52**, 214.
10. Talekar, V. L. and Rawat, S. S., *J. Inst. Telecomn. Engrs.*, 1971, **17**, 334.
11. Gupta, R. K., *Indian J. Radio Space Phys.*, 1972, **1**, 281.

NEWS

HELP FOR FATIGUE FROM ALPHA INTERFERON

. . . "Recombinant alpha interferons have . . . shown activity in many forms of leukemia and lymphoma. Tachyphylaxis [decreasing responses following repeated injections] to the acute toxic effects (fevers, rigors, myalgias, headache, and so forth) occurs with the first few doses, but fatigue and anorexia are often persistent and progressive, requiring substantial reductions in the dose or even cessation of therapy. We postulated that the typical hospital or clinic routine of morning injections, with serum interferon levels peaking in the afternoon, might be partially responsible for the fatigue encountered, since even mild or unnoticeable symptoms could produce the 'washed out' feeling that patients often described. In addition, we found that patients did not always sleep well at night after being fatigued and sleepy during the day. We are currently conducting several studies employing recombinant alpha interferon (Roferon) at doses ranging from 3 million units daily to 50 million units per square meter of body-surface area three times a week. After tachyphylaxis to the acute toxic effects, we began treating patients in the evening. Approximately 75% of all the patients, and 90% of those taking the low daily dose, reported an improvement in their energy level, as compared with that experienced by patients taking interferon during the day. . . . We believe that evening administration of alpha interferon is preferable for patients and may be applicable to other biologic response modifiers in which fatigue is a major toxic effect."

[(Paul G. Abrams et al. (Natl. Cancer Inst.) in *New England Journal of Medicine* 312(7):443-4, 14 Feb 85 (Letter to the editor)). Reproduced with permission from Press Digest, *Current Contents*®, No. 15, April 15, 1985, p. 15, (Published by the Institute for Scientific Information®, Philadelphia, PA, USA.)]